Nonparabolicity of the conduction band in GaAs

T. Ruf and M. Cardona
Max-Planck-Institut für Festkörperforschung, Heisenbergstrasse 1, Postfach 80 06 65, D-7000 Stuttgart 80, Federal Republic of Germany
(Received 31 January 1990)

The technique of resonant Raman scattering is used in a magnetic field to determine interband magneto-optical transitions in GaAs(001) from enhancements of the 1-LO- and 2-LO-phonon intensities due to resonances with Landau levels. The experiments were performed far above the E_0 fundamental gap, where corrections due to Coulomb effects can be neglected. We observed incoming, outgoing, and intermediate resonances involving only heavy-mass valence levels. These levels can be described rather accurately by solving an 8×8 $\mathbf{k}\cdot\mathbf{p}$ matrix with 30 Pidgeon-Brown blocks, and therefore, the observed nonlinearities in the fan plots of laser energy $\hbar\omega_l$ versus magnetic field B for transitions with Landau quantum numbers n can be attributed to the nonparabolicity of the Γ_6^c conduction band of GaAs. A simple formula for the bulk Γ_6^c dispersion is deduced from a two-band model with only one parameter to fit the fan plots for different scattering configurations and types of resonances. This yields an experimental determination of the conduction-band dispersion and effective mass in the region from 100 meV up to about 300 meV above the E_0 fundamental gap. Our results compare favorably with 16×16 $\mathbf{k}\cdot\mathbf{p}$ and pseudopotential calculations.

I. INTRODUCTION

Resonant Raman scattering has been used recently to study electronic structure and electron-phonon interaction in strong magnetic fields. The quantization of electronic states into Landau orbits leads to resonant enhancement of Stokes LO-phonon Raman lines when the incident laser energy is kept fixed and the magnetic field is varied such that either incident or scattered photon energies (or both at the same time) match with interband magneto-optical transitions of bulk III-V compound semiconductors like GaAs or InP. These phenomena, referred to as incoming, outgoing, and double resonances, have been studied both experimentally and theoretically.[1,2] It was also discovered that the presence of a magnetic field enhances the efficiency of higher-order Raman scattering and magneto-Raman profiles for scattering by up to 4 LO phonons have been obtained.[3]

In the original work by Ambrazevičius *et al.*[4] pronounced nonlinearities in the fan plot obtained from magneto-Raman profiles were attributed to conduction-band nonparabolicity, and a satisfactory description of the experiment could only be achieved with the introduction of an additional constant C^* from higher- and remote-band contributions. Even though that work covered a rather wide range of energies with profiles taken at only a few laser energies, it provided clear evidence that resonant Raman scattering in high magnetic fields can be used advantageously to investigate the electronic structure of III-V compound semiconductors.

In this work we present a thorough investigation of the nonparabolicity of the Γ_6^c conduction band in GaAs(001) which gives full justice to recent developments in the field such as selection rules and scattering mechanisms for different scattering configurations, admixed valence-level structure, and resonances of outgoing or incoming character.[1,2]

In Sec. II the theoretical framework is discussed. An analytical expression for the conduction-band nonparabolicity is presented and approximations made to interpret magneto-Raman data are discussed. Section III gives the results obtained from 1-LO- and 2-LO-phonon profiles. From this the bulk dispersion of the conduction band and the effective-mass–versus–energy relation are obtained. The conclusions of this work are given in Sec. IV. In the Appendix the validity of our approximation for the conduction-band dispersion is discussed, particularly the effect of additional terms arising in a five-level $\mathbf{k}\cdot\mathbf{p}$ scheme.

II. THEORY

The electronic structure of III-V compound semiconductors in the presence of external magnetic fields can be described quite accurately within the framework of $\mathbf{k}\cdot\mathbf{p}$ theory. Starting from the description given by Luttinger and Kohn[5,6] who gave an analytical solution for the admixed valence-level (Γ_8^v) structure by diagonalizing 2×2 matrices, Pidgeon and Brown[7] extended the theory to treat the interaction between conduction and valence bands exactly. This turned out to be necessary since the fundamental gaps in most III-V compound semiconductors are not sufficiently large compared to other typical energies (such as spin-orbit splittings, Landau-level energies) to treat them by perturbation theory. In fact, for most purposes, an accurate description of the conduction bands in these materials within $\mathbf{k}\cdot\mathbf{p}$ theory is only possible using the 14 (or 16) states from the Γ_7^s, Γ_8^v, Γ_6^c, Γ_7^c, and Γ_8^c (Γ_1') manifolds.[8,9] Invariant analyses of Pidgeon-Brown–type 8×8 $\mathbf{k}\cdot\mathbf{p}$ Hamiltonians have been per-

formed for elemental[10] and III-V compound semiconductors,[11] and Landau levels determined from them were used successfully to identify intraband and interband magneto-optical transitions from far-infrared transmission, modulated reflectivity, and resonant magneto-Raman experiments.

One of the most useful applications of magneto-optical studies has always been the determination of band parameters.[12,13] The treatment of the Landau-level structure of a III-V compound semiconductor in an 8×8 or even 16×16 $\mathbf{k}\cdot\mathbf{p}$ scheme with a complicated mixing in the valence levels and many terms which have to be considered makes a numerical fit to experimental fan plots a rather cumbersome task. The more effective approach is to extract information from physically meaningful approximations with only a few parameters to be adjusted. In our investigation on the nonparabolicity of the Γ_6^c conduction band in GaAs, we proceed just this way.

The energies of resonances which are observed in magneto-Raman profiles have several contributions. The E_0 fundamental gap accounts for most of the interband transition energy. Electron and hole Landau levels reflect the respective bulk dispersions. Coulomb effects lead to a lowering of the transition energies and the incoming or outgoing character of the resonances has to be taken into account by shifting the transition energies by the energy corresponding to the number of phonons emitted before the resonant transition occurs.

In GaAs(001) for exciting laser energies $\hbar\omega_l$ above ≈1700 meV only resonances which involve heavy-mass valence levels ($10\lesssim n\lesssim30$) are observed in our experiments. Due to their large mass as compared to that of the electrons, they contribute rather little to the interband transition energies. Nevertheless, they have to be treated as accurately as possible if one wants to extract information on one particular set of levels such as those from the Γ_6^c conduction manifold. Previous magneto-Raman experiments were interpreted using heavy-mass levels calculated with the 8×8 $\mathbf{k}\cdot\mathbf{p}$ scheme from Ref. 11.[2] For the theoretical computation of magneto-Raman profiles, the analytical formulas given by Luttinger[6] were shown to be sufficient to describe the dominant features observed in a region of energies close to double resonance.[1,2] In that work, which was limited to laser energies $\hbar\omega_l\lesssim1700$ meV and thus to Landau quantum numbers $n\lesssim10$, the agreement between the two calculations is better than the experimental accuracy of about 1 meV at 12 T. For larger Landau quantum numbers, however, deviations between the eigenenergies calculated with Luttinger's expressions and the more elaborate theory[11] become evident. In Fig. 1 we show the behavior of several heavy-mass Landau levels with magnetic field. The dashed lines correspond to values calculated with the analytical formulas,[6] whereas the solid lines represent values obtained from the diagonalization of the Hamiltonian given by Trebin und Rössler, where 30 8×8 $\mathbf{k}\cdot\mathbf{p}$ blocks were considered. We chose the $|n,\ J=\frac{3}{2},\ J_z=\pm\frac{1}{2}\rangle$ admixtures of the eigenstates to represent the heavy-mass levels since they dominate the wave functions in the limit of large n. It can be seen that the fan lines obtained from the more accurate model do not increase

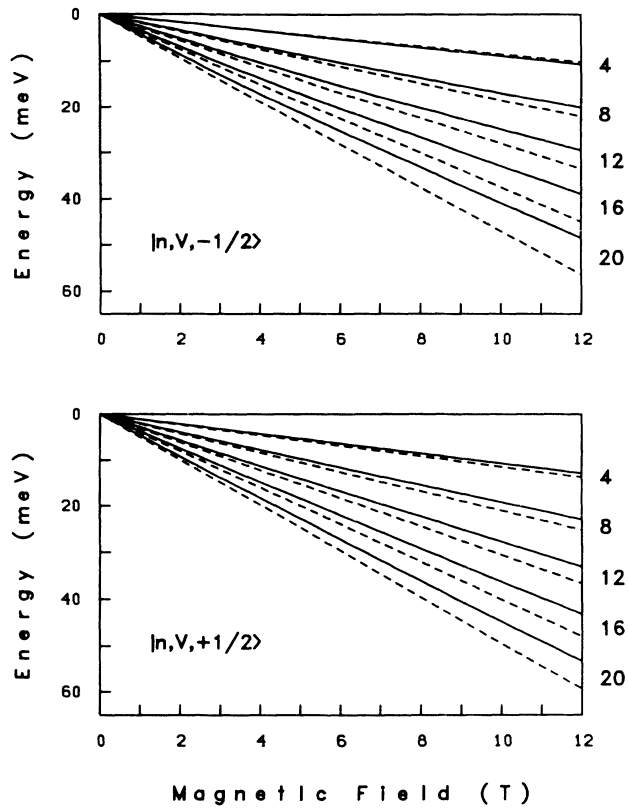

FIG. 1. Comparison of heavy-mass Landau levels calculated with two models. Solid lines: eigenenergies from the diagonalization of a matrix with 30 8×8 $\mathbf{k}\cdot\mathbf{p}$ Pidgeon-Brown–type blocks (Ref. 11). Dashed lines: calculation with the analytical expressions given by Luttinger (Ref. 6). The eigenstates $|n,\ V,\ \pm\frac{1}{2}\rangle$ stand for the dominant admixtures of the wave functions in the limit of large n. Landau indices are given to the right of the figures. For clarity, not all Landau levels are shown.

with magnetic field as rapidly as suggested by the linear solutions of the 2×2 approximation. Deviations from linearity manifest themselves in a bending towards lower energies which becomes more pronounced for larger Landau quantum numbers n and amounts to more than 5 meV for $n=20$ at 12 T. The differences in Landau-level energies between the two calculations arise from the fact that an isotropic valence band was assumed in Luttinger's calculations, whereas the hole anisotropy is fully considered in the 8×8 calculation. The latter is roughly equivalent to averaging the heavy-hole masses along the [100] and [110] directions. Results in good agreement with the solid lines of Fig. 1 can be obtained by solving the 2×2 problem with mean values of $\gamma'(\gamma_2,\gamma_3)$ and $\gamma''(\gamma_2,\gamma_3)$ for the two directions.[6] This has to be taken into account when subtracting hole contributions from interband transition energies. Otherwise, the nonparabolicity of the conduction band will be incorrectly increased.

The electron Landau levels in a III-V compound semiconductor were treated by Braun and Rössler.[14] They performed an invariant expansion of the $\mathbf{k}\cdot\mathbf{p}$ Hamiltonian up to fourth order in k and identified the expansion coefficients (material and band parameters) by compar-

ison with the expression obtained in perturbation theory up to the same order in k. Focusing on the nonparabolicity of the conduction band, we chose a different approach. In a two-band approximation,[15] taking an average value $E_0^* = E_0 + \Delta_0/3$ to account for spin-orbit interaction, the $\mathbf{k}\cdot\mathbf{p}$ Hamiltonian for conduction and valence bands can be written as

$$\mathcal{H} = \frac{\hbar^2 k^2}{2m_0}(1+C^*)\cdot 1 + \begin{bmatrix} E_0^*/2 & (\hbar/\sqrt{2m_0})kP \\ (\hbar/\sqrt{2m_0})kP & -E_0^*/2 \end{bmatrix} . \quad (1)$$

Here the origin of the energy scale was taken to be in the middle of the spin-orbit-averaged E_0^* fundamental gap. kP interactions are included as off-diagonal elements, representing a coupling between valence and conduction bands via the momentum matrix element P as defined in Refs. 9 and 16. The nonparabolicity of the conduction band shall be described by the additional term proportional to the constant C^*, which has to be adjusted by comparison with the experiment. The physical significance of this term will become evident after diagonalization of the above Hamiltonian, which for the energy above the bottom of the conduction band yields the following expression, isotropic in $\mathbf{k}$:[4]

$$E(k) = -\frac{E_0^*}{2} + \left[\left(\frac{E_0^*}{2} \right)^2 + \frac{\hbar^2 k^2}{2m_0} P^2 \right]^{1/2} + \frac{\hbar^2 k^2}{2m_0}(1+C^*) . \quad (2)$$

Expanding this expression for small k and keeping terms up to fourth order in k gives

$$E(k) \simeq \frac{\hbar^2 k^2}{2m_0}\left[1 + \frac{P^2}{E_0^*} + C^*\right] - \left[\frac{\hbar^2 k^2}{2m_0}\right]^2 \frac{P^4}{E_0^{*3}} . \quad (3)$$

We take

$$\frac{1}{m_e^*} = \frac{1}{\hbar^2 k}\frac{dE(k)}{dk} \quad (4)$$

as a definition of the dynamical effective mass, i.e., that which enters the semiclassical equation of motion under the action of an external force. The effective mass at the bottom of the conduction band is given by

$$\frac{m_0}{m_{e0}^*} = 1 + \frac{P^2}{E_0^*} + C^* . \quad (5)$$

Comparing Eq. (5) with the expression given in Ref. 16, the nonparabolicity constant C^* can be connected to contributions from the higher conduction bands Γ_7^c and Γ_8^c, represented by the matrix element P',[9] and from more remote Γ_{15}-like bands. The remote-band contributions are commonly included in a constant C.[8,16] Nonparabolicity effects are contained in the k^4-terms of Eq. (3). The validity of this approach to describe the conduction band of GaAs is discussed in the Appendix. Identifying kinetic energies with cyclotron orbits by translating all terms $\hbar^2 k^2/2m_0$ in Eq. (2) into $(\hbar eB/m_0 c)(n+\frac{1}{2})$ as magnetic energies[13] and fixing the band-edge mass according to Eq. (5), the expression which will be used to fit the experimental magneto-Raman fan plots reads[4]

$$E(n,B) = -\frac{E_0^*}{2} + \left[\left(\frac{E_0^*}{2} \right)^2 + E_0^* \left(\frac{m_0}{m_{e0}^*} - 1 - C^* \right) \frac{\hbar eB}{m_0 c}(n+\tfrac{1}{2}) \right]^{1/2} + \frac{\hbar eB}{m_0 c}(1+C^*)(n+\tfrac{1}{2}) . \quad (6)$$

It is easy to see by differentiating Eq. (6) with respect to n that in the limit of large n and $(\hbar eB/m_0^* c)(n+\frac{1}{2})/E_0^* \ll 1$ the difference $E(n,B) - E(n-1,B) = \hbar eB/m_e^* c$ with m_e^* given by Eq. (4) for $k^2 = 2eBn/\hbar c$, as expected on physical grounds.

In previous magneto-Raman and interband magneto-optical studies, the effect of Coulomb interactions between electrons and holes had to be taken into account as a correction to transition energies, depending on the magnetic field and on the Landau quantum number n.[2,17] The variational approach for the exciton binding energy presented in Ref. 17 can be used to demonstrate that the effect of Coulomb interactions decreases for large Landau quantum numbers n. In the regime of large n, where our experiments were performed, it can be neglected.

Magneto-Raman data taken close to the E_0 fundamental gaps of InP (Ref. 17) and GaAs (Ref. 2) were interpreted in terms of outgoing resonances involving either light or heavy-mass levels. The analysis of the dominant contributions to the Raman efficiency shows, however, that in the region far above the E_0 fundamental gap incoming resonances with heavy-mass levels take over for GaAs.[2] The onset of such behavior has been found in recent experiments. In the 1-LO-phonon data, which are presented in the following section, the change from outgoing to incoming resonances will be demonstrated and different parts of the fan plots will be assigned to the different types of resonances.

Fan plots obtained from magneto-Raman profiles at the spectral positions corresponding to 2 LO phonons exhibit a slightly different behavior. Whereas the fan lines for laser energies closest to E_0 can be attributed to outgoing resonances (i.e., after the emission of 2 LO phonons) with light-mass levels, the high-energy regions display

resonances which for $B \rightarrow 0$ head towards $E_0+(1\ \mathrm{LO})$. This indicates that these resonances are of the *intermediate* type. They are found to involve heavy-mass valence levels. The theoretical origin of this behavior still has to be investigated.

III. EXPERIMENT

The experimental procedure to measure the intensity of Raman scattering as a function of the magnetic field has been described before.[4,17] Here it suffices to say that in these experiments resonant Raman scattering is used as a kind of modulation spectroscopy with an internal modulation applied to the semiconductor under investigation by its characteristic vibrational modes. This internal modulation allows for a highly sensitive determination of interband magneto-optical transitions. In the present study we make use of this property to investigate the electronic structure of GaAs up to 300 meV above the E_0 fundamental gap. The sample under study was a (001) surface of GaAs prepared by liquid-phase epitaxy, the same sample as in Ref. 4.

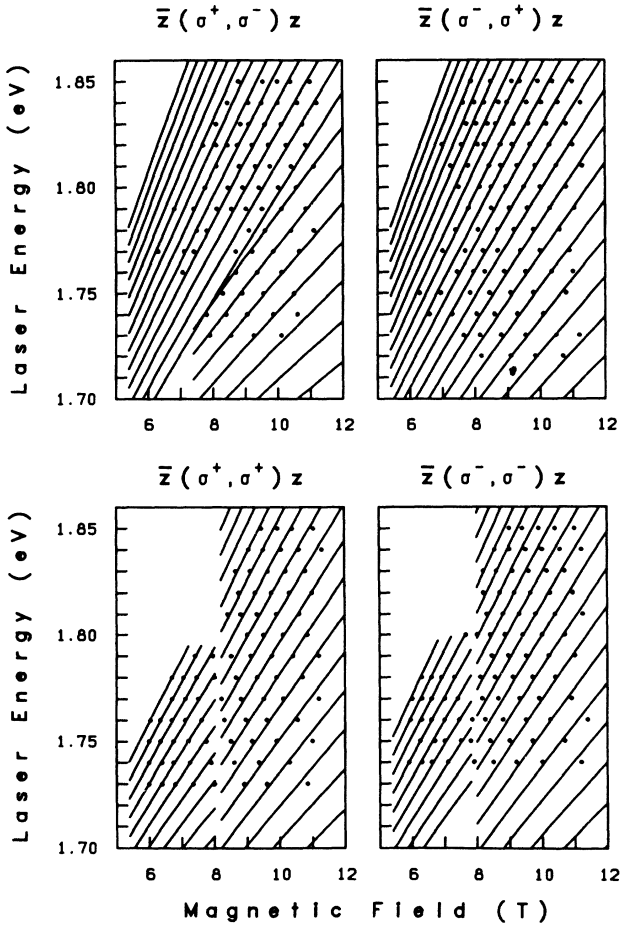

FIG. 2. Magneto-Raman fan plots for different scattering configurations obtained from resonances in the scattering by 1 LO phonon. The solid lines indicate theoretical fan plots in incoming and outgoing resonance which give the best agreement with the experiment (see text). Values of C^* determined from this and information on the fan lines plotted are given in Table I.

Figure 2 shows fan plots of resonances in 1-LO phonon Raman scattering consisting of plots of laser energy at which resonances occur versus magnetic field. The positions of fan lines in the various scattering configurations with circularly polarized light[1] reflect selection rules for interband transitions between Landau levels and other electronic properties such as hole g factors. The solid lines were obtained theoretically using Eq. (6) for the energies of the conduction-band Landau levels. The contribution from heavy-mass levels was incorporated according to the solid lines in Fig. 1. The same Luttinger and other band parameters were used as in Refs. 1 and 2 to calculate the valence levels using an 8×8 $\mathbf{k}\cdot\mathbf{p}$ matrix with 30 Pidgeon-Brown–type blocks. For all fits the band-edge conduction-electron effective mass was taken to be $m_{e0}^*=0.0665m_0$.[18] This value is in good agreement with determinations from both interband absorption[19] and cyclotron resonance.[20] A slightly smaller value for m_{e0}^* was obtained by Sigg *et al.*, who performed a cyclotron-resonance study taking band non-parabolicity and polaron corrections into account.[21] According to dipole selection rules for interband transitions in the Faraday configuration ($\mathbf{B}\| \mp\mathbf{k}_{\mathrm{light}}$), resonances in σ^+ polarization were assigned to transitions between $|n, V, J_z=-\frac{1}{2}\rangle$ heavy-mass levels and $|n,\uparrow\rangle$ conduction states, while σ^- transitions were taken to couple $|n, V, J_z=+\frac{1}{2}\rangle$ hole states to $|n,\downarrow\rangle$ conduction levels. The arrows $\uparrow$ ($\downarrow$) stand for electron Landau levels with spin up (down). In most of the scattering configurations, a distinction between outgoing resonances for smaller laser energies and magnetic fields and incoming resonances in the high-field and high-excitation-energy case can be made. These

TABLE I. Summary of the experimental determinations of the nonparabolicity constant C^* from (a) 1-LO-phonon and (b) 2-LO-phonon magneto-Raman profiles for different scattering configurations and types of resonances. The ranges of Landau quantum numbers n for which theoretical fan lines are plotted in Figs. 2 and 3 are also given.

(a) Fan plots from 1-LO-phonon magneto-Raman profiles

Scattering configuration	Type of resonance	C^*	Landau n of fan lines plotted in Fig. 2
$\bar{z}(\sigma^+,\sigma^-)z$	incoming	-1.90	$16\le n\le 28$
	outgoing	-2.85	$7\le n\le 13$
$\bar{z}(\sigma^-,\sigma^+)z$	incoming	-2.40	$9\le n\le 28$
$\bar{z}(\sigma^+,\sigma^+)z$	incoming	-2.00	$9\le n\le 24$
	outgoing	-2.65	$10\le n\le 19$
$\bar{z}(\sigma^-,\sigma^-)z$	incoming	-2.00	$9\le n\le 25$
	outgoing	-2.15	$12\le n\le 20$

(b) Fan plots from 2-LO-phonon magneto-Raman profiles

Scattering configuration	Type of resonance	C^*	Landau n of fan lines plotted in Fig. 3
$\bar{z}(\sigma^+,\sigma^-)z$	intermediate	-2.35	$7\le n\le 28$
$\bar{z}(\sigma^-,\sigma^+)z$	intermediate	-2.65	$7\le n\le 28$
$\bar{z}(\sigma^+,\sigma^+)z$	intermediate	-2.45	$8\le n\le 28$
$\bar{z}(\sigma^-,\sigma^-)z$	intermediate	-2.50	$8\le n\le 28$

different parts of the fan plots were separately used to determine the nonparabolicity constant C^*. Results from the fits are summarized in Table I. The fan lines in the $\bar{z}(\sigma^+,\sigma^-)z$ configuration were assigned to outgoing resonances in the lower right-hand side of the corresponding fan plot. The upper part of the plot reveals incoming resonances which for $B\rightarrow 0$ converge to the E_0 fundamental gap. In the $\bar{z}(\sigma^-,\sigma^+)z$ configuration only incoming resonances are observed. The different regions of incoming and outgoing resonances in the other two configurations can be easily distinguished by the steeper slope exhibited by the incoming fan lines compared to the outgoing ones. The ranges of Landau-level numbers n for which theoretical fan lines are plotted in Fig. 2 are also given in Table I. The various fan plots were calculated as described above using the respective values of C^* given in Table I.

Figure 3 shows the fan plots obtained from magneto-Raman profiles at 2 LO phonons. The values of C^* determined from these results are summarized in Table I(b). In all scattering configurations the fan lines had to be assigned to intermediate resonances involving heavy-mass levels. Thus for $B\rightarrow 0$ they converge at $E_0+(1$ LO). In the two scattering configurations with equal circular polarizations no data points are shown for magnetic fields larger than about 8 T. In that region a complex structure of fan lines is found that could not be definitely assigned to any type of resonance. Further investigations in the frame of multiphonon magneto-Raman scattering are necessary.

It should be mentioned that the data from Ref. 4 give a value of $C^*=-1.95$ when fitted with the approach presented in this work. Upon comparing this value to $C^*=-3.2$ as obtained in Ref. 4, the necessity of using accurate energies for the heavy-mass levels becomes evident; otherwise, the nonparabolicity is artificially increased. Taking an average over all determined values of C^*, we find $C^*=-2.3\pm0.3$ The dispersion of the Γ_6^c conduction band obtained with Eq. (2) using this value of C^* and $m_{e0}^*=0.0665m_0$ is shown in Fig. 4. The solid line with the error bars (from $\Delta C^*=\pm0.3$) represents the experimentally determined dispersion up to 300 meV above the bottom of the band. The dashed line gives the parabolic limit for that value of m_{e0}.* The experimental dispersion determined from our experiments can be reproduced using the 16×16 $\mathbf{k}\cdot\mathbf{p}$ expansion given in Ref. 9 when P' is adjusted accordingly. With $P'=5.1$ eV Å ($\hat{=}0.354$ a.u.) and the parameters from Ref. 9, the dotted curves in the inset of Fig. 4 are obtained for the [100] and [110] directions. Note that the only change in parameters as compared to Ref. 9 is an increase in P' by about 6%. The dispersion according to Eq. (2) with the experimental value of C^* is given by the solid line in the inset of Fig. 4. One finds that even though the experimental

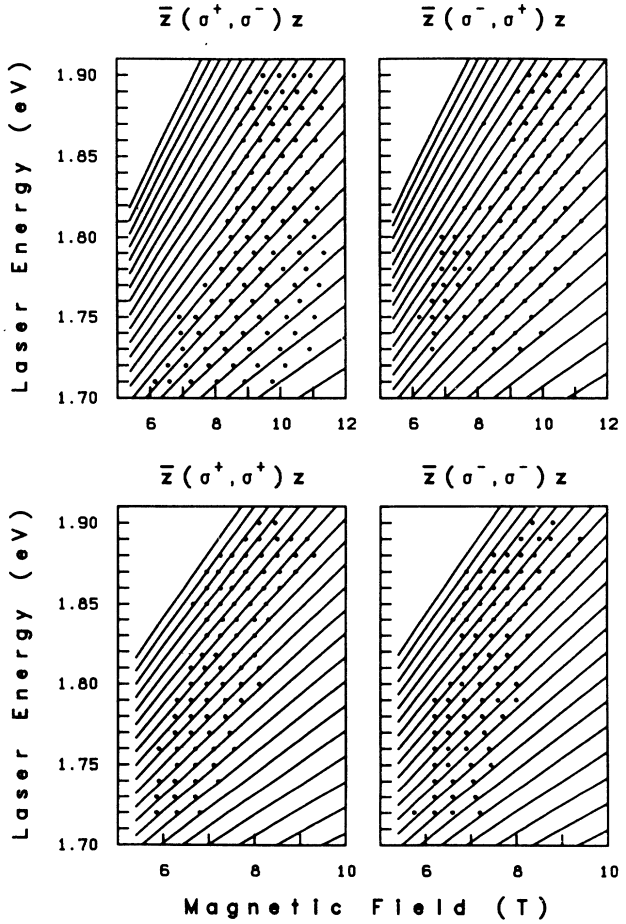

FIG. 3. Magneto-Raman fan plots and theoretical fits for different scattering configurations from 2-LO-phonon scattering. See text and Table I for further information.

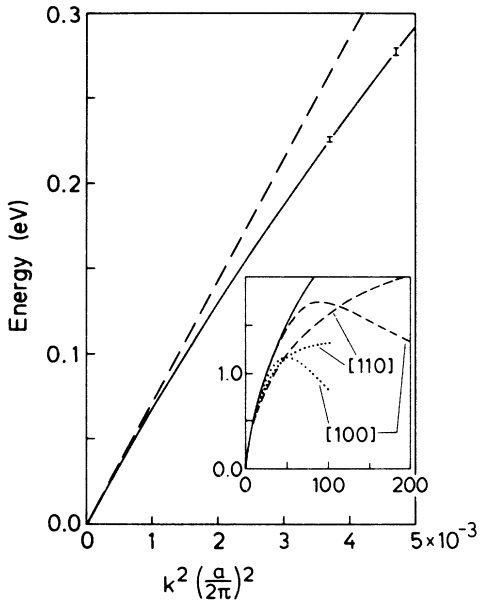

FIG. 4. Dispersion of the Γ_6^c conduction band in GaAs(001). The solid line was calculated using Eq. (2) with $C^*=-2.3\pm0.3$ and $m_{e0}^*=0.0665m_0$. The dashed line gives the parabolic dispersion for that m_{e0}^*. In the inset our result (solid line) is compared with dispersions obtained from a 16×16 $\mathbf{k}\cdot\mathbf{p}$ Hamiltonian (dotted curves) and from a local empirical pseudopotential calculation (dashed curves) in the [100] and [110] directions.

data are limited to about 300 meV above the band edge, the agreement between our experimental results, fitted with a simple two-band model, and the solution of the more sophisticated 16×16 **k p** Hamiltonian is excellent for energies up to 600 meV above the bottom of the band, which corresponds to 10% of the Brillouin zone in the Γ–X direction. The dashed lines in the inset of Fig. 4 originate from local empirical pseudopotential calculations for the indicated directions, performed with a cutoff of 6 Ry, which corresponds to a basis set of about 59 plane waves.[22] Parameters and form factors were taken from Ref. 23. The dispersion for the [100] direction also agrees with our experimental result up to 0.6 eV. Even though it is not possible to distinguish between the [100] and [110] directions within the experimental accuracy in the range up to 300 meV above the bottom of the conduction band, it turns out that the experimental dispersion found by adjusting C^*, when extrapolated to values of E higher than 0.6 eV, is closer to that for the [100] direction rather than to an average value in the (001) plane. We believe that this effect is fortuitous and due to the breakdown of Eq. (2) at these energies.

To compare our result with more conventional treatments of conduction-band nonparabolicity it is suitable to express the dispersion in the form[8]

$$E(k) \simeq \frac{\hbar^2 k^2}{2m_{e0}^*} + \alpha_0 k^4 , \tag{7}$$

neglecting other contributions of order k^3 like the small inversion-asymmetry-induced spin splitting[9] and k^4 anisotropy. With our parameters and Eq. (3), we find a value of $\alpha_0 = -2370 \pm 100$ eV Å^4 as compared to the estimate of $\alpha_0 = -1969$ eV Å^4 given by Braun and Rössler in Ref. 14. Interband experiments to determine the conduction-band nonparabolicity in GaAs are rather scarce, but a study which comes close to the method used here has been performed by Suemoto *et al.*,[24] who used resonant Raman scattering to determine the energies of conduction subbands in wide *p*-type modulation-doped $Al_xGa_{1-x}As$-GaAs-AlAs quantum wells. Bulk parameters and effective masses from the 16×16 **k·p** Hamiltonian of Ref. 9 were taken to describe the electrons confined to the GaAs well. The quantum wells used in these experiments were rather wide (about 700 Å), and thus one should expect them to reflect the *bulk* band structure. Comparing the energy dispersion of the conduction-subband levels from that work with our results, we find that there are still deviations from the bulk dispersion due to confinement effects even in such wide wells. The additional bending there is about the same as that due to bulk conduction-band nonparabolicity. In Fig. 5 we show the conduction-band effective mass calculated from Eq. (4) with the dispersion from Eq. (2) and the experimental parameters. The solid line with error bars for $\Delta C^* = 0.3$ represents the experimental result, whereas the dashed line originates from the solution of the 16×16 **k·p** Hamiltonian with the change in P' mentioned earlier. The lower solid line was calculated with $C^* = 0$, i.e., neglecting contributions from higher conduction (Γ_{15}) and more remote bands.

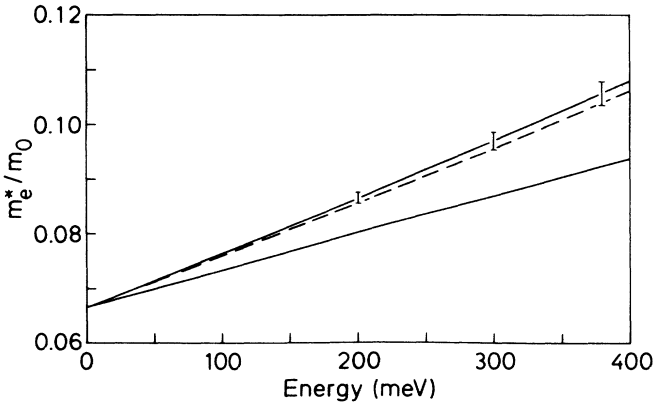

FIG. 5. Conduction-band effective mass of GaAs(001) vs energy above the bottom of the band. The solid line with error bars represents the experimental result with $m_{e0}^* = 0.0665 m_0$ and $C^* = -2.3 \pm 0.3$. The dashed line is obtained when the dispersion from a 16×16 **k·p** Hamiltonian is fitted to the experimental dispersion. The lower solid line was calculated with $C^* = 0$.

IV. CONCLUSIONS

Resonance profiles from magneto-Raman scattering at 1 LO phonon and 2 LO phonons have been analyzed to determine the nonparabolicity of the Γ_6^c conduction band in GaAs(001). Fan lines in incoming, intermediate, and outgoing resonances were assigned to interband magneto-optical transitions using a dispersion relation derived from a two-band model. Fits of this simple theory (one parameter) to the data give an experimental determination for the conduction-band dispersion up to 300 meV above the bottom of the band. The nonparabolicity observed is in agreement with more sophisticated **k·p** and pseudopotential calculations, and the two-band model describes the dispersion as far as 10% away from the center of the Brillouin zone. In GaAs the dominant contribution in the conduction-band nonparabolicity arises from terms proportional to $P^4/(E_0^*)^3$, and other contributions may be neglected. The most important additional contribution to the effective mass in a five-level model arises from terms proportional to $(P')^2$.

ACKNOWLEDGMENTS

We are pleased to thank H. Hirt, M. Siemers, and P. Wurster for first class technical assistance. Thanks are due to S. Zollner for kindly providing his pseudopotential calculations prior to publication and to G. Fasol for discussions on the 16×16 **k·p** program. U. Rössler provided **k·p** results, which are gratefully acknowledged. Thanks are due to D. Heitmann for a critical reading of the manuscript.

APPENDIX

The description of the conduction band of GaAs with the two-band model of Sec. II and the consideration of higher conduction and more remote bands via the constant C^* is not *a priori* obvious, even though the expan-

sion of Eq. (3) up to fourth order in k yields the conventional contributions[16] to the dispersion $E(k)$. From a more thorough analysis, taking the higher Γ_{15}^c conduction band into account, one should expect contributions of order k^4 which arise from the interaction of the Γ_1 conduction band with Γ_{15}^v and Γ_{15}^c valence and conduction bands, represented by matrix elements P and P'.[14] To that order, processes involving coupling between Γ_{15}^v and Γ_{15}^c (matrix element Q) should also contribute.[14] The latter terms vanish for k along the [001] direction, but one has to keep in mind that the cyclotron orbits for $\mathbf{B}\|[001]$ actually sample an average of the electronic properties of both the [100] and [110] directions.

In order to incorporate the contribution of [110] directions in a two-band model we choose a set of basis functions of symmetry $X+Y$, $X-Y$, and Z to represent the Γ_{15}^v valence band. Treating the above couplings in second-order perturbation theory and neglecting part of the resulting 4×4 matrix, a matrix for the $\{S, X+Y\}$ manifold, omitting factors of $\hbar^2/(2m_0)$, can be written as

$$\mathcal{H}=\begin{bmatrix} E_0^*/2-\{(P')^2/[(E_0')^*-E_0^*]\}k^2 & kP-\{P'Q/[(E_0')^*-E_0^*]\}\cdot k^2 \\ kP-\{P'Q/[(E_0')^*-E_0^*]\}\cdot k^2 & -E_0^*/2-[Q^2/(E_0')^*]k^2 \end{bmatrix}. \tag{A1}$$

To account for spin-orbit coupling, the energies of E_0 and E_0' critical points have to be replaced by the averaged values of $E_0^*=E_0+\Delta_0/3=1.631$ eV and $(E_0')^*=E_0'+2\Delta_0'/3=4.602$ eV. Introducing the constants $\tilde{C}=-(P')^2/[(E_0')^*-E_0^*]$ and $\hat{C}=-Q^2/(E_0')^*$, the conduction-band dispersion reads

$$E(k)=-\frac{E_0^*}{2}+\left[\tfrac{1}{4}[E_0^*+(\tilde{C}-\hat{C})k^2]^2+\left[kP-\frac{P'Q}{(E_0')^*-E_0^*}k^2\right]^2\right]^{1/2}+[1+\tfrac{1}{2}(\tilde{C}+\hat{C})]k^2, \tag{A2}$$

with the origin of energy at the bottom of the band. An expansion up to $O(k^4)$ gives

$$E(k)=\left[1+\frac{P^2}{E_0^*}+\tilde{C}\right]k^2-\frac{2P'QP}{E_0^*[(E_0')^*-E_0^*]}k^3-\left[\frac{P^4}{(E_0^*)^3}+\frac{P^2(\tilde{C}-\hat{C})}{(E_0^*)^2}-\frac{(P')^2Q^2}{E_0^*[(E_0')^*-E_0^*]^2}\right]k^4. \tag{A3}$$

With parameters for GaAs (Ref. 9) [$P^2=26$ eV, $(P')^2=6$ eV, $Q^2=12$ eV], one obtains values of $\tilde{C}=-2.0$ and $\hat{C}=-2.6$. The other terms proportional to k^4 contribute only 0.6% of $P^4/(E_0^*)^3$ to the nonparabolicity. Therefore the nonparabolicity is dominated by the $P^4/(E_0^*)^3$ term and, due to the fact that $\tilde{C}\simeq\hat{C}$, we find that Eq. (A3) reduces to the form given in Eq. (3) when the small k^3 contributions along the [110] direction are neglected. In other III-V compound semiconductors these additional contributions to the nonparabolicity do not necessarily cancel and, e.g., in InP they give a contribution of 7% compared to $P^4/(E_0^*)^3$ using the parameters of Ref. 9. While this is still small, one may have to use Eq. (A2) instead of Eq. (3) when more precise magneto-Raman data for that material become available.

[1] C. Trallero-Giner, T. Ruf, and M. Cardona, Phys. Rev. B **41**, 3028 (1990).
[2] T. Ruf, R. T. Phillips, C. Trallero-Giner, and M. Cardona, Phys. Rev. B **41**, 3039 (1990).
[3] T. Ruf and M. Cardona, Phys. Rev. Lett. **63**, 2288 (1989).
[4] G. Ambrazevičius, M. Cardona, and R. Merlin, Phys. Rev. Lett. **59**, 700 (1987).
[5] J. M. Luttinger and W. Kohn, Phys. Rev. **97**, 869 (1955).
[6] J. M. Luttinger, Phys. Rev. **102**, 1030 (1956).
[7] C. R. Pidgeon and R. N. Brown, Phys. Rev. **146**, 575 (1966).
[8] U. Rössler, Solid State Commun. **49**, 943 (1984).
[9] M. Cardona, N. E. Christensen, and G. Fasol, Phys. Rev. B **38**, 1806 (1988).
[10] K. Suzuki and J. C. Hensel, Phys. Rev. B **9**, 4184 (1974).
[11] H.-R. Trebin, U. Rössler, and R. Ranvaud, Phys. Rev. B **20**, 686 (1979).
[12] R. L. Aggarwal, Phys. Rev. B **2**, 446 (1970).
[13] M. Reine, R. L. Aggarwal, and B. Lax, Phys. Rev. B **5**, 3033 (1972).
[14] M. Braun and U. Rössler, J. Phys. C **18**, 3365 (1985).
[15] E. O. Kane, in *Semiconductors and Semimetals*, edited by R. K. Willardson and A. C. Beer (Academic, New York, 1966), Vol. 1, p. 75.
[16] C. Hermann and C. Weisbuch, Phys. Rev. B **15**, 823 (1977).
[17] T. Ruf, R. T. Phillips, A. Cantarero, G. Ambrazevičius, M. Cardona, J. Schmitz, and U. Rössler, Phys. Rev. B **39**, 13378 (1989).
[18] *Physics of Group IV Elements and III-V Compounds*, Vol. 17a of *Landolt-Börnstein*, edited by O. Madelung, M. Schulz, and H. Weiss (Springer-Verlag, Berlin, 1982).
[19] Q. H. F. Vrehen, J. Phys. Chem. Solids **29**, 129 (1968).
[20] M. A. Hopkins, R. J. Nicholas, M. A. Brummell, J. J. Harris, and C. T. Foxon, Phys. Rev. B **36**, 4789 (1987).
[21] H. Sigg, P. Wyder, and J. A. A. J. Perenboom, Phys. Rev. B **31**, 5253 (1985).
[22] S. Zollner (private communication).
[23] J. P. Walter and M. L. Cohen, Phys. Rev. **183**, 763 (1969).
[24] T. Suemoto, G. Fasol, and K. Ploog, Phys. Rev. B **37**, 6397 (1988).